Improved illumination system for spatial coherence control

Zhiqiang Liu,[1,*] Takashi Gemma,[1] Joseph Rosen,[2] and Mitsuo Takeda[3]

[1]Optical Technology Development Department, Core Technology Center, Nikon C/O. 1-6-3, Nishi-ohi 1-chome, Shinagawa-ku, Tokyo 140-8601, Japan

[2]Department of Electrical and Computer Engineering, Ben-Gurion University of the Negev, P.O. Box 653, Beer-Sheva 84105, Israel

[3]Department of Information and Communication Engineering, The University of Electro-Communications, 1-5-1, Chofugaoka, Chofu, Tokyo 182-8585, Japan

*Corresponding author: liu.zq@nikon.co.jp

Received 2 November 2009; accepted 5 January 2010;
posted 28 January 2010 (Doc. ID 119328); published 12 February 2010

An improved illumination system is proposed for creating a temporally coherent and spatially incoherent extended source to be used for spatial coherence control and reconstruction of a coherent hologram. Taking into account the fact that a rotating ground glass does not behave as an ideal Lambertian diffuser, the new illumination system tailors the directivity of the scattered lights to direct the lights efficiently into an interferometer so that a spatial coherence function can be better controlled and detected with higher fidelity. Experimental results are presented that demonstrate improved performance of the proposed system. © 2010 Optical Society of America

OCIS codes: 030.1640, 120.1088.

1. Introduction

One of major obstacles in high-precision laser interferometry is so-called coherent noise or an artifact fringe pattern, which arises from spurious interference of lights scattered by dust and defects on optical surfaces, as well as lights reflected from surfaces of optical elements other than the test surface. To reduce the effect of the unwanted noise fringes while maintaining the contrast of the desired signal fringes localized on the object surface to be probed, use has been made of short temporal coherence of a broadband light source, as exemplified by white-light interferometry [1] and optical coherence tomography [2]. However, the wide spread of the spectrum introduces uncertainty into the exact wavelength of the light to be used as the length scale. Moreover, the broadband light gives rise to a dispersion problem, particularly when the system includes refractive optical elements or the measurement is made through a dispersive medium. For this reason, use of monochromatic light is highly desirable, provided a means is available that can solve the coherence noise problem.

Rosen and Takeda [3] proposed a technique in which spatial coherence is adaptively controlled by using a variable extended spatially incoherent quasi-monochromatic source created by a spatial light modulator (SLM). A similar technique was also proposed by Kuecher [4] and Deck *et al.*[5] to suppress the coherence noise. Wang *et al.* [6] gave a new interpretation to the principle of the Rosen–Takeda scheme [3] and verified it by experiment. Duan *et al.* [7] and Gokhler *et al.* [8] further developed this method and applied it to profilometry, while Baleine and Dogariu [9] applied the spatial coherence control technique to variable coherence tomography. Ryabukho *et al.* [10,11] studied longitudinal coherence for a light field with wide frequency and angular spectra. More recently, Takeda *et al.* [12] proposed

0003-6935/10/160D12-05$15.00/0

and experimentally demonstrated a more general technique, called coherence holography, which can synthesize an arbitrary 3-D spatial coherence function.

The key component that plays a crucial role in these techniques is the extended quasi-monochromatic light source with a specified irradiance distribution and the unique characteristic that it is temporally coherent and yet spatially incoherent. To realize this special characteristic, the specified source pattern (representing a Fresnel-zone-plate-like pattern or a coherence hologram) is displayed on an SLM. The source pattern on the SLM is illuminated with a collimated laser beam and imaged onto a rotating ground glass that destroys the spatial coherence of the laser light while maintaining its temporal coherence. Implicit in the theory of our previous papers [3,6,8,12] is that the ground glass is an ideal Lambertian diffuser that scatters the light uniformly in all directions. However, this is not the case, and in reality a ground glass exhibits a strong directivity of scattering in the direction of the incidence beam. For this reason, the coherence function cannot be controlled exactly as predicted from the theory.

In this paper, we propose a new illumination system to remove the influence of the directivity of the ground glass. By using this illumination system, the coherence function can be controlled according to the theory even when the ground glass has strong directivity. First, we explain the principle of our illumination system, and then we show experimental results to demonstrate the advantage of our illumination system.

2. Principle

For convenience of explanation, we use an example of the optical system described in Ref. [3]. Figure 1 shows an optical setup used for longitudinal spatial coherence control. In Fig. 1, S is a point on the rotating ground glass, onto which a zone-plate-like source pattern displayed on the SLM (not shown in the figure) is imaged to create a spatially incoherent and temporally coherent light source. Light from the point source S is collimated by a lens L3 of focal length f. The collimated light illuminates the test and reference surfaces M1 and M2, where M1 is the projected virtual mirror of a real test mirror located above the beam splitter (not shown in Fig. 1), and the beams reflected from these surfaces interfere on a CCD image sensor. Lens L4 is used to image the test surface onto the CCD.

Generally, the intensity of light scattered by the ground glass is not uniform, and the light is directed strongly in the direction of the incident illuminating beam. Schematically, Fig. 2 shows a typical example of the scattering characteristic of a ground glass, where the lengths of the arrows represent the brightness of the scattered light and θ is the angle between the incident ray and the scattered ray. If we take into account the scattering directivity function $P(\theta)$, the field distribution on mirror M1 can be written as

$$u(x,y,z) = \frac{u_s(x_s,y_s)}{j\lambda f}P(\theta) \times \exp\left[j\frac{2\pi(z+2f)}{\lambda} - j\frac{2\pi}{\lambda f}(x_s x + y_s y) - j\frac{\pi z}{\lambda f^2}(x_s^2 + y_s^2)\right], \quad (1)$$

where λ is the wavelength, $j = \sqrt{-1}$, (x,y,z) are the coordinates of the observation point with their origin at the rear focus of L3, and $u(x_s,y_s)$ is the complex amplitude of the scattered light at a point (x_s,y_s) on the ground glass.

The scattering directivity function $P(\theta)$ in Eq. (1) can be rewritten by the geometrical parameters of the illuminating system defined in Fig. 3. In Fig. 3, f is the focal length of the collimator lens L3, and s is the distance between lens L3 and the test surface. The ground glass is illuminated by a point source at A, located at a distance a from the collimator lens L3. The ray passing through the ground glass without being scattered forms an image of the point source A at another point B on the optical axis through lens L3; b is the distance from lens L3 to point B.

Let us note one ray in the illumination beam that reaches the ground glass at x_s, where only a meridian ray height x is considered because the illumination is rotationally symmetric. The ray passes through the ground glass directly (without being scattered) and is bent by lens L3 to meet the test surface at x_t and to cross the optical axis at point B. Therefore, we have

$$x_t = x_s\frac{a}{a-f}\cdot\frac{b-s}{b}. \quad (2)$$

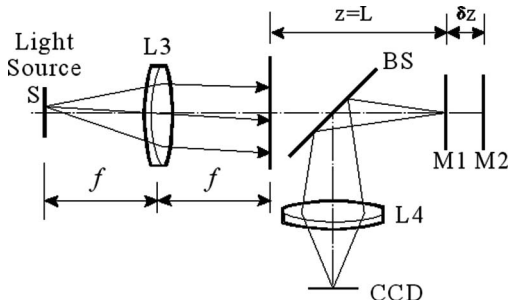

Fig. 1. Optical setup for coherence control.

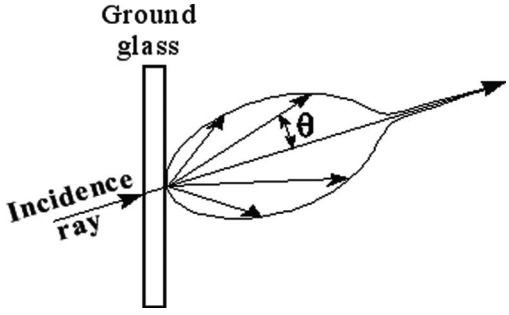

Fig. 2. Typical scattering characteristic of a ground glass.

Since the ground glass is placed at the front focal plane of lens L3, the light scattered at (x_s, y_s) is collimated by lens L3. Therefore, θ can be written as

$$\theta = \frac{x - x_t}{f}, \tag{3}$$

where x is the height of the ray scattered at angle θ. Note that generally $P(\theta)$ is not a constant function because θ is related to (x_s, y_s) through Eqs. (2) and (3). Therefore, the intensity distribution of the fringes cannot be calculated directly from the formula given in our previous papers [3,6,8,12]. In order to make the actual system meet the theory, we propose an additional condition for the illumination system.

We form the image of the point source A on the test surface such that

$$b = s, \tag{4}$$

which makes $x_t = 0$. Then, because of the axial symmetry of the optical system, Eq. (3) becomes

$$\theta = \frac{r}{f} = \frac{\sqrt{x^2 + y^2}}{f}. \tag{5}$$

The field distribution described by Eq. (1) becomes

$$u(x,y,z) = \frac{u_s(x_s,y_s)}{j\lambda f} p\left(\frac{\sqrt{x^2+y^2}}{f}\right) \times \exp\left[j\frac{2\pi(z+2f)}{\lambda} - j\frac{2\pi}{\lambda f}(x_s x + y_s y) - j\frac{\pi z}{\lambda f^2}(x_s^2 + y_s^2)\right]. \tag{6}$$

In this field distribution, scattering directivity function $P(\theta)$ has now become independent from the coordinates (x_s, y_s). Implicit in this derivation is an assumption that the scattering directivity function $P(\theta)$ does not change its function form significantly. Because the light source is spatially incoherent, the intensity of the interferogram on CCD is given by the superposition of the fringe intensity created by the individual point sources.

$$I(x,y,L) = \left[p\left(\frac{\sqrt{x^2+y^2}}{f}\right)\right]^2 \iint \left| \frac{u_s(x_s,y_s)}{j\lambda f} \times \exp\left[j\frac{2\pi(L+2f)}{\lambda} - j\frac{2\pi}{\lambda f}(x_s x + y_s y) - j\frac{\pi L}{\lambda f^2}(x_s^2 + y_s^2)\right] + \frac{u_s(x_s,y_s)}{j\lambda f} \times \exp\left[j\frac{2\pi(L+2\Delta z+2f)}{\lambda} - j\frac{2\pi}{\lambda f}(x_s x + y_s y) - j\frac{\pi(L+2\Delta z)}{\lambda f^2}(x_s^2 + y_s^2)\right]\right|^2 dx_s dy_s, \tag{7}$$

where L is the distance between the ground glass plate and the test surface and δz is the optical distance between the test and reference surfaces.

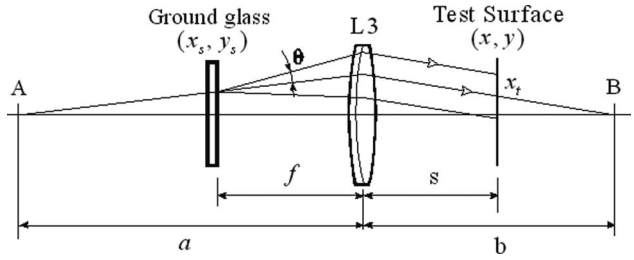

Fig. 3. Illumination system.

Now the directivity of the ground glass appears only as a nonuniform intensity distribution observed on the measured object surface. Accordingly, the validity of the coherence controlling theory can be maintained even when the ground glass has a scattering function with a strong directivity.

As a specific example, let us consider a special case in which the ground glass is illuminated with a collimated beam from a point source A located at infinity. Rays passed by the ground glass without being scattered are focused on the rear focus of the collimation lens L3. According the proposed illumination condition, the object surface should be placed in the rear focal plane of lens L3 to satisfy the requirement $b = f$. Under this condition, one can use Eq. (7) for the field distribution on the test surface.

3. Experiment

We conducted an experiment to demonstrate the improved performance of the proposed illumination system. A schematic illustration of the optical setup is shown in Fig. 4. A beam from a He–Ne laser with wavelength 632.8 nm is expanded by an objective lens Ob and a lens L0 to illuminate the SLM and is focused at point A by relay lenses L1 and L2 to form a secondary point source. This beam is spatially modulated to have the zone-plate-like intensity distribution displayed on SLM. The zone-plate-like pattern displayed on the SLM is imaged onto a rotation ground glass by lenses L1 and L2. Lenses L1 and L2 have the same focal length of ~18 mm. The distance between the two lenses is ~162 mm. A rotating ground glass is placed in the front focal plane of lens L3 with focal length ~81 mm. Accordingly light scattered from a point on the ground glass is collimated by lens L3. A beam splitter, BS, separates the light into two beams, of which one is directed to test mirror M1 (which functions as a virtual mirror M1 in Fig. 1) and the other to reference mirror M2. The test and reference beams are reflected by mirrors M1 and

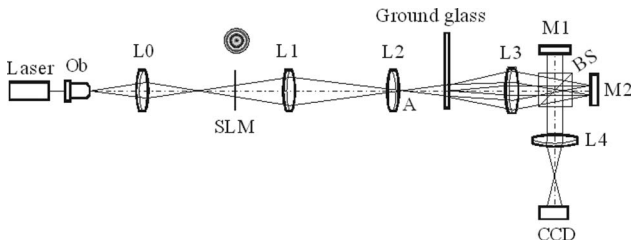

Fig. 4. Experimental setup.

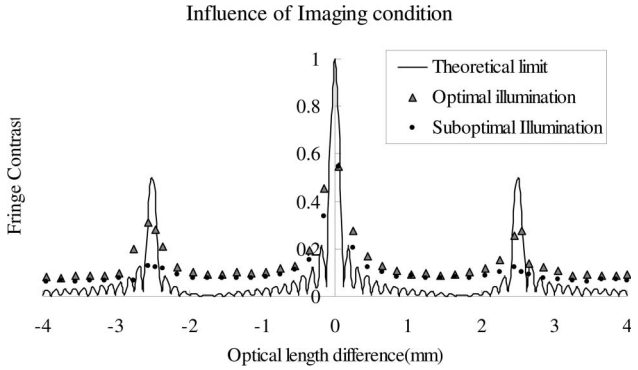

Fig. 5. Longitudinal spatial coherence function.

M2, respectively, and interfere on the CCD. Lens L4 images mirror surface M1 on the CCD.

In this experiment, the zone-plate-like source displayed on SLM was adjusted such that the longitudinal coherence function has a high peak when the axial distance between mirror M1 and mirror M2 is $\delta z = 2.5\,\text{mm}$. In this experiment, the number of zone-plate rings N was chosen to be 20 to meet the limit of the ground glass size. In this particular condition, light from an arbitrary point in the bright zone rings generates a fringe pattern with the same phase when mirror M1 and are separated by 2.5 mm. Consequently, the diameter S_{ZP} of the zone-plate-like source pattern on the rotating ground glass should be

$$D_{\text{ZP}} = 2f \times \tan\left[\arccos\left(1 - \frac{N\lambda}{2t}\right)\right] \approx 2f\sqrt{\frac{N\lambda}{t}} = 11.54\,\text{mm}, \tag{8}$$

where the approximation $\tan[\arccos(1 - x/2)] \approx \sqrt{x}$ holds for $0 \le x \ll 1$. In our system, the diameter of lens L3 is $D_{\text{L3}} = 48\,\text{mm}$, and the distance from the point A to the rotating ground glass is $l_{\text{A-G}} = 111.2\,\text{mm}$. Therefore, the diameter of the maximum measurable area on the test surface (which is defined as the area for which all the light scattered from the circular source area of diameter D_{ZP} on the ground glass is guaranteed to reach on the test surface) is limited to

$$d = 2\left(\frac{D_{\text{L3}}}{2} - \frac{l_{\text{A-G}} + f}{l_{\text{A-G}}} \times \frac{D_{\text{ZP}}}{2}\right) = 28.0\,\text{mm}, \tag{9}$$

where we have assumed the scattering directivity function $P(\theta)$ does not vanish for the scatter angle $\theta \le \arctan(0.5d/f)$.

We shifted mirror M2 in such a way that the axial distance between mirror M2 and the virtual image of mirror M varies from −4 mm to 4 mm. We measured the fringe contrast of the interferogram at each mirror position; the result is shown in Fig. 5, together with the coherence function predicted by theory. For the comparison of performance, we shifted the location of the point source A so that the illumination system is made to deviate from the prescribed condition; this resulted in the shift of point B by 120 mm from mirror M1. The coherence function in this case is also measured and shown in Fig. 5. In Fig. 5, the horizontal axis shows the distance between the test and reference mirror. The vertical axis shows the visibility of the interferograms. An example of interferograms is shown in Fig. 6, where (a), (b), and (c) correspond to the distances of the reference and test mirror being zero, 1.5 mm and 2.5 mm, respectively.

For the illumination system optimally designed according to our theory, the longitudinal coherence function has high peaks when the test and reference mirror is separated 2.5 mm as shown by the triangles in Fig. 5. The coherence peaks have overlapping tails. Therefore, the peak heights should be made as high as possible by the proposed technique to avoid the influence of the tails on the detected peak position. The coherence peak height becomes lower when the point B is shifted from mirror M1, and the prescribed illumination condition is not satisfied. The coherence function is shown by circles in Fig. 5. This result demonstrates the validity of our illumination condition.

Even in the optimal illumination, the peak height of the coherence function is lower than that predicted by theory. This may be caused by the intensity

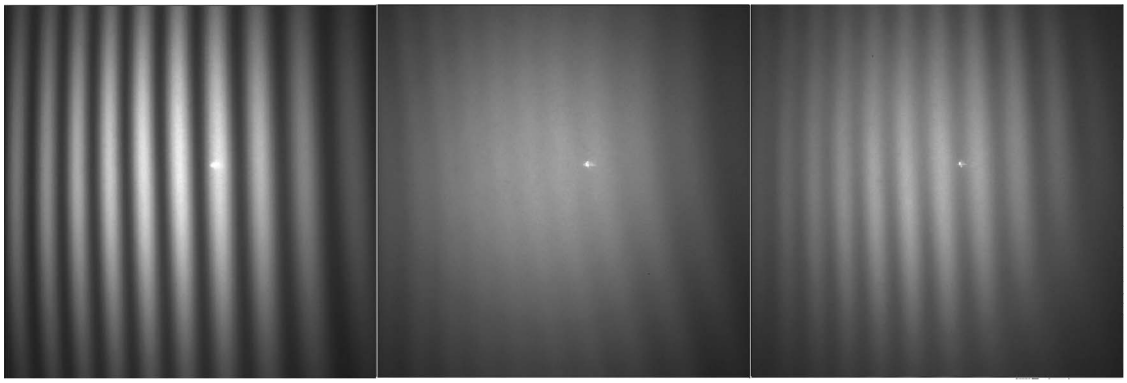

Fig. 6. Interferograms for the distances between the reference and test mirrors being (a) 0 mm, (b) 1.5 mm, and (c) 2.5 mm.

imbalance between the object and signal beams in the interferometer, the nonuniform illumination of the SLM and the aberrations of the illumination system.

4. Conclusions

To improve the performance of the coherence control technique, we proposed a new design principle for the illumination system. The new design can reduce the influence of the scattering directivity of the ground glass. We carried out an experiment and demonstrated the advantage of our illumination system. For better control of the coherence function, the aberration of the illumination system and the nonuniform illumination of SLM must be reduced.

References

1. P. A. Flournoy, R. W. McClure, and G. Wyntjes, "White-light interferometric thickness gauge," Appl. Opt. **11**, 1907–1915 (1972).
2. D. Huang, E. A. Swanson, C. P. Lin, J. S. Schuman, W. G. Stinson, W. Chang, M. R. Hee, T. Flotte, K. Gregory, C. A. Puliafito, and J. G. Fujimoto, "Optical coherence tomography," Science **254**, 1178–1181 (1991).
3. J. Rosen and M. Takeda, "Longitudinal spatial coherence applied for surface profilometry," Appl. Opt. **39** , 4107–4111 (2000).
4. M. Kuechel, " Apparatus and method(s) for reducing the effect of coherent artifacts in an interferometer," U.S. patent 6,804,011 (22 January 2002).
5. L. L. Deck, D. Stephenson, E. Gratix, and C. A. Zanoni, "Apparatus and method(s) for reducing the effect of coherent artifacts in an interferometer," U.S. patent 6,643,024 (3 May 2001).
6. W. Wang, H. Kozaki, J. Rosen, and M. Takeda, "Synthesis of longitudinal coherence functions by spatial modulation of an extended light source: a new interpretation and experimental verification," Appl. Opt. **41**, 1962–1970 (2002).
7. Z. Duan, M. Gokhler, J. Rosen, H. Kozaki, N. Ishii, and M. Takeda, "Synthesis spatial coherence function for optical tomography and profilometry: simultaneous realization of longitudinal coherence scan and phase shift," Proc. SPIE **4777**, 110–177 (2002).
8. M. Gokhler, Z. Duan, J. Rosen, and M. Takeda, "Spatial coherence radar applied for tilted surface profilometry," Opt. Eng. **42**, 830–836 (2003).
9. E. Baleine and A. Dogariu, "Variable coherence tomography," Opt. Lett. **29**, 1233–1235 (2004).
10. V. Ryabukho, D. Lyakin, and M. Lobachev, "Influence of longitudinal spatial coherence on the signal of a scanning interferometer," Opt. Lett. **29**, 667–669 (2004).
11. V. Ryabukho, D. Lyakin, and M. Lobachev, "Longitudinal pure spatial coherence of a light field with wide frequency and angular spectra," Opt. Lett. **30**, 224–226 (2005).
12. M. Takeda, W. Wang, Z. Duan, and Y. Miyamoto, "Coherence holography," Opt. Express **13**, 9629–9635 (2005).